Focused Laser Differential Interferometer Response to a Controlled Phase Object

A. Hameed[*] N. J. Parziale[†]

Stevens Institute of Technology, Hoboken, NJ 07030, USA

In this paper, we characterize the response of the focused laser differential interferometer (FLDI) instrument to a controlled phase object. A thin, uni-directional, controlled phase object is created by vibrating a cylindrical lens in the beam path. Attached to this lens is an accelerometer from which displacement may be measured and, with knowledge of the lens geometry, the phase response of a differential interferometer may be calculated. We compare the phase response derived from the accelerometer to that measured by the FLDI. This accelerometer-derived phase change was found to be in excellent agreement with the FLDI-derived phase change for both single and double FLDI setups with different phase-object strengths (focal lengths) in both amplitude and frequency.

$\Delta\phi$	= Phase change, (radians)
λ	= Laser wavelength, (m)
L	= Length, (m)
R	= Radius of curvature of lens, (m)
n	= Index of refraction, (-)
Δx	= Beam intraspacing, (m)
V	= Voltage, (V)
ρ	= Density, (kg/m^3)
κ	= Wavenumber, (1/m)

Subscript
a	= Ambient
g	= Glass

I.   Introduction

Understanding the phenomenon of high-speed boundary layer transition is important for the development of hypersonic vehicles. The high velocities, stagnation temperatures, and broad ranges of length and time scales present unique challenges in studying these flows using traditional experimental techniques and numerical simulations. Established flow diagnostic techniques include pressure transducers, hot-wire anemometers, and heat flux gauges. Each of these traditional measurement techniques have unique limitations: hot-wire anemometers are encumbered by wire breakage, limited frequency response, flow intrusion, and signal interpretation problems; heat flux gauges and pressure transducers have limited bandwidth and are restricted to on-surface measurements. Non-intrusive optical diagnostic techniques have recently gained popularity, their appeal promoted by recent improvements in imaging, electronics, and laser technology.[1]

Focused laser differential interferometry (FLDI) is a novel nonparticle-based optical flow diagnostic technique pioneered by Smeets[2–7] and Smeets and George[8] in the 1970s. In the 1980s/1990s/2000s, other researchers have used laser differential interferometry (LDI) to make measurements in high-speed flows.[9–14] More recently, Parziale et al.[15–21] used the FLDI technique to characterize facility disturbance level and boundary-layer instability and transition in the Caltech T5 reflected-shock tunnel. Since that time re-

---

*Graduate Student, Mechanical Engineering, Castle Point on Hudson, Hoboken, New Jersey, 07030.
†Associate Professor, Mechanical Engineering, Castle Point on Hudson, Hoboken, New Jersey, 07030, Senior AIAA Member.

searchers have made additional advancements including making reliable convective velocity measurements between two closely spaced FLDI probe volumes,[22–29] facility disturbance-level characterization,[30–32] and novel beam shaping techniques for application in hard-to-access flows.[33–37] Additionally, researchers have devised controlled problems[38–40] to test the data-reduction strategies by Fulghum,[41] Settles and Fulghum,[42] and Schmidt and Shepherd.[43]

The objective of this work is to characterize the response of the FLDI instrument to a controlled phase object. We measure the response of an FLDI instrument to an oscillating optical path length and compare it to the vibrations measured by an accelerometer. This is a calibration in both amplitude and frequency.

II.   Experimental Setup

A basic FLDI setup is developed by first expanding a linearly polarized laser beam using a diverging lens. The expanding beam is then circularly polarized by a quarter-wave plate before being split into two beams of mutually orthogonal, linear polarization by a Wollaston prism. The diverging beams are collimated by locating the Wollaston prism at the focal point (or close to) of a converging lens. The converging lens brings the beams to a focus. When the beams are recombined by a second Wollaston prism and linear polarizer, they interfere with one another. The interference is measured by a change in intensity on a photodetector.

The FLDI is sensitive to the phase difference between the beam pairs of the instrument. The phase difference between a beam pair is due to the separate optical path lengths traversed by the individual beams in the FLDI setup. Unwanted signals are rejected by the FLDI outside of the focus area by filtering due to finite beam separation, finite beam width, and beam overlap.

This basic FLDI setup can be expanded by the addition of quarter-wave plates and Wollaston prisms upstream of the focus to generate additional beam pairs, and corresponding photodetectors downstream of the focus to measure their interference. In this work, a single beam pair FLDI setup and a double beam pair D-FLDI setup was utilized. The components of the D-FLDI setup are shown in Fig. 1.
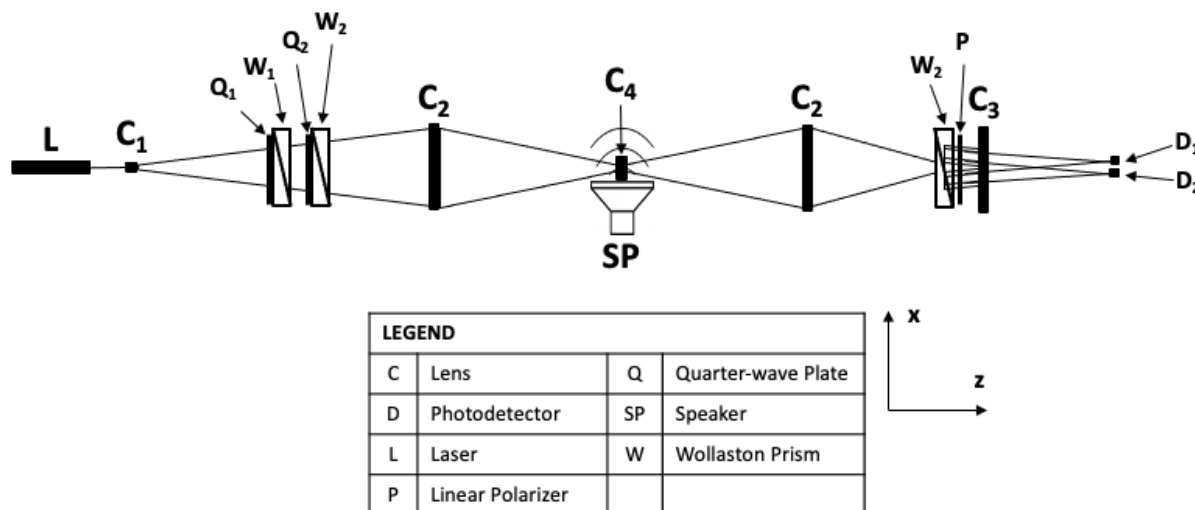
Figure 1: Schematic of a D-FLDI setup. C_1 is the diverging lens used to expand the linearly polarized laser beam. The upbeam quarter-wave plate (Q_1, Q_2) and Wollaston prism (W_1, W_2) generate the two beam pairs in a D-FLDI setup. C_2 is the converging lens used to focus the beams. The downbeam Wollaston prism (W_2) and linear polarizer (P) recombine the beams within each beam pair. Another lens (C_3) is used to separate the beams so that they can be focused onto photodetectors. A single point FLDI setup is developed by removing one of the the upbeam quarter-wave plate and Wollaston prism bundles. C_4 represents the lenses used as phase objects in these experiments.

For this experiment, an FLDI instrument was constructed using a Wollaston prism with a 1-arcminute splitting angle and a D-FLDI instrument was constructed by adding a Wollaston prism with a 20-arcminute splitting angle. For both the FLDI and D-FLDI setups, the beams were inter- and intraspaced in the

$x-$ direction. For the FLDI setup, an intraspacing of 41.063 μm is achieved. For the D-FLDI setup, an intraspacing of 40.984 μm and an interspacing of 699.242 μm was achieved. Pictures of the beams at the focus for both setups are shown in Fig. 2.
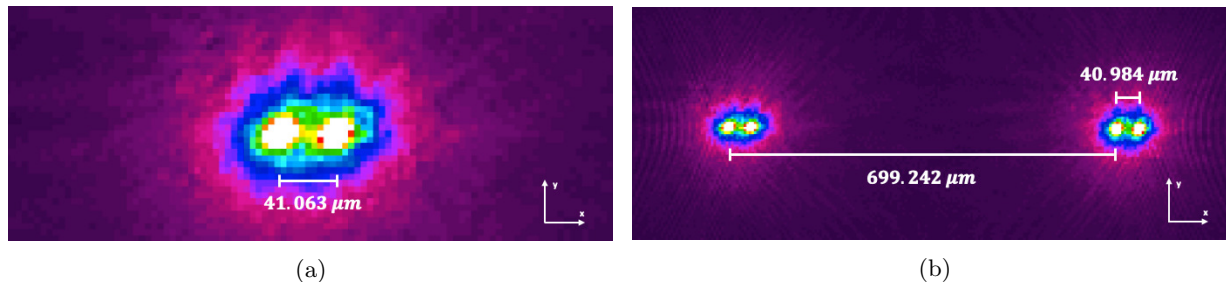
Figure 2: Pictures of (a) FLDI and (b) D-FLDI beam pairs taken at the focus using an Ophir-Spirion LT665 beam profiling camera. To capture the closely intraspaced beams in each setup, the camera's aperture was reduced to 5 ms.

To measure the response of the FLDI setup to a changing optical path length, the apparatus pictured in Fig. 3 was constructed. The apparatus was mounted on a manually adjustable translation stage and consisted of a speaker, an accelerometer, and a cylindrical diverging lens as a phase object. The setup could be precisely adjusted in the $\pm z$-direction using a translation stage. The speaker was driven at a prescribed frequency by a Stanford Research Systems model DS345 synthesized function generator. The diverging lens was suspended by a compliant spring directly in front of the speaker. The radius of curvature of the lens was along the direction of beam separation. The lens was positioned such that it gently touched the speaker, and it was placed in the path of the FLDI beams. As the speaker was driven at the prescribed frequency, its vibrations oscillated the lens along the direction of beam separation, changing the individual lengths traversed by each FLDI beam. A PCB 352C34 accelerometer measured the apparatus's acceleration and was mounted directly to the lens, in-line with the direction of oscillation.

For the single point FLDI setup, a cylindrical diverging lens of -50 mm was used as the phase object. For the D-FLDI setup, weaker lenses of focal lengths -150 mm and -400 mm were used to reduce beam steering and distortion. Initially, the apparatus was placed such that the lens was at the point of best focus of the FLDI beams, i.e. $z = 0$. As the speaker was vibrated at the driving frequency, a comparison was made between the frequency measured by the FLDI instrument and the accelerometer, and between the amplitude of the phase change as measured by the FLDI instrument and as calculated using the accelerometer.

Figure 3: Apparatus used to measure the response of the FLDI instrument to a changing optical path length.

The apparatus described above modeled a density disturbance field experienced by an FLDI instrument that is sinusoidal in x, uniform in y, and infinitesimally thin in z, of the form $\rho = \rho(x, y, z) = \sin(\kappa x)\delta(z)$.

III.   Phase Change Due to Cylindrical Lens Displacement

Similar to Ceruzzi et al.,[24] the optical path lengths (OPLs) of two FLDI beams as they pass through a lens of radius of curvature R is shown in Fig. 4. The phase difference experienced by the FLDI beam pairs of

wavelength λ due to their distinct optical paths is

$$\Delta\phi = \frac{2\pi}{\lambda}\Delta OPL = \frac{2\pi}{\lambda}\left((L_1 n_a + L_3 n_g) - (L_2 n_a + L_4 n_g)\right), \tag{1}$$

where ΔOPL represents the difference in optical path lengths between the individual beam pairs, L is distance, n_g is the refractive index of the glass, and n_a is the refractive index of the ambient environment.
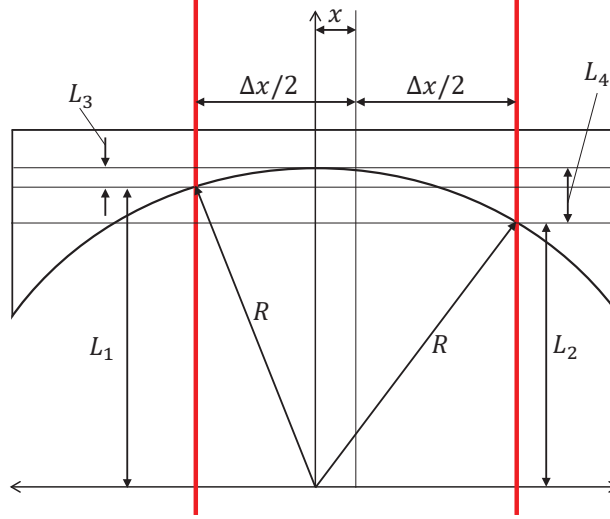
Figure 4: Cylindrical lens of radius of curvature R with FLDI beams (red) displaced by Δx. The center of the FLDI beams are displaced a distance x from the origin.

The lengths can be found in terms of the geometry of the optical setup as

$$L_1^2 + (\Delta x/2 - x)^2 = R^2, \tag{2a}$$

$$L_2^2 + (\Delta x/2 + x)^2 = R^2, \tag{2b}$$

$L_3 = R - L_1$, and $L_4 = R - L_2$.

Simplifying the above relations results in

$$\Delta\phi = \frac{2\pi}{\lambda}\left[(n_g - n_a)\left(\sqrt{R^2 - (\Delta x/2 - x)^2} - \sqrt{R^2 - (\Delta x/2 + x)^2}\right)\right], \tag{3}$$

which enables the calculation of phase change if the position, x, of the lens is known. We determine the position with an accelerometer, which may be independently compared to the phase change from the FLDI signal as

$$\Delta\phi = \sin^{-1}\left(\frac{V}{V_0} - 1\right), \tag{4}$$

where V_0 is the voltage at the most linear part of a fringe. It is obtained by averaging the minimum and maximum voltage output of the FLDI instrument measured by a photodetector as the downstream Wollaston prism is adjusted to translate the FLDI instrument through a fringe.

IV.   Results and Discussion

In this section, we compare the phase change as measured by the FLDI instrument and the accelerometer. Results from an experiment with an FLDI setup and a $f_L = $-50 mm focal length cylindrical diverging lens phase object placed at the focus are presented first. The FLDI beam pair is shown in this position in

Fig. 2a. Fig. 5-left shows the acceleration, velocity, and position of the phase object as measured by the accelerometer. The acceleration, $a(t)$, is numerically integrated once in the time domain to obtain the velocity, $v(t)$, and again to obtain the position, $x(t)$. Alternatively, the position of the phase object can be obtained in frequency space by pre-multipication of the FFT of the acceleration data as $\mathcal{F}[a(t)]/(4\pi^2 f^2)$. Comparison of the two methods are presented in Fig. 5-right, and represent a sanity check. Moreover, the amplitude of the fundamental frequency in $|x(f)|$ at 50 Hz matches the observed amplitude in Fig. 5-left.
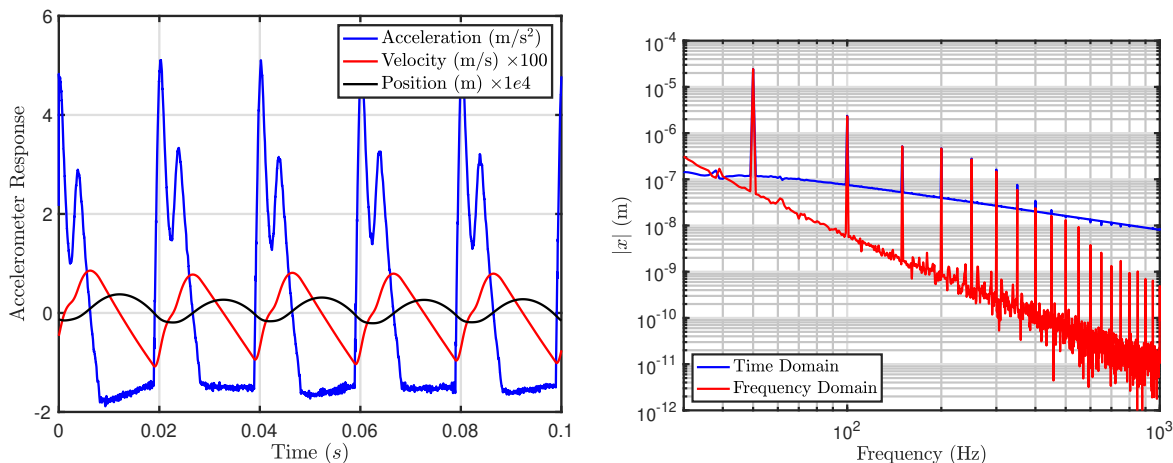
Figure 5: Left: Acceleration, velocity and position of the phase object as measured by the accelerometer; velocity and position are obtained by numerical integration. Right: FFT of the position of the lens as computed by the numerical integration of accelerometer data (Time Domain) and as computed by the pre-multipication of the FFT of the acceleration data, $\mathcal{F}[a(t)]/(4\pi^2 f^2)$, (Frequency Domain).

The position, $x(t)$, of the lens, calculated from the accelerometer signal is substituted into Eq. (3) to directly obtain the phase change, $\Delta\phi$, as measured by the accelerometer. The phase change as measured by the FLDI instrument is determined by substituting the voltage output of the photodetector, $V(t)$, into Eq. (4). Results for the phase change as measured by the accelerometer and the FLDI instrument for this experiment are presented in Fig. 6-left. To obtain the spectrum of the phase change from the accelerometer data we input $|x(f)| = \mathcal{F}[a(t)]/(4\pi^2 f^2)$ into Eq. (3). We present a comparison of the accelerometer-derived and FLDI-derived phase-change spectrum as Fig. 6-right noting excellent agreement at the fundamental frequency (50 Hz) and a half dozen harmonics.
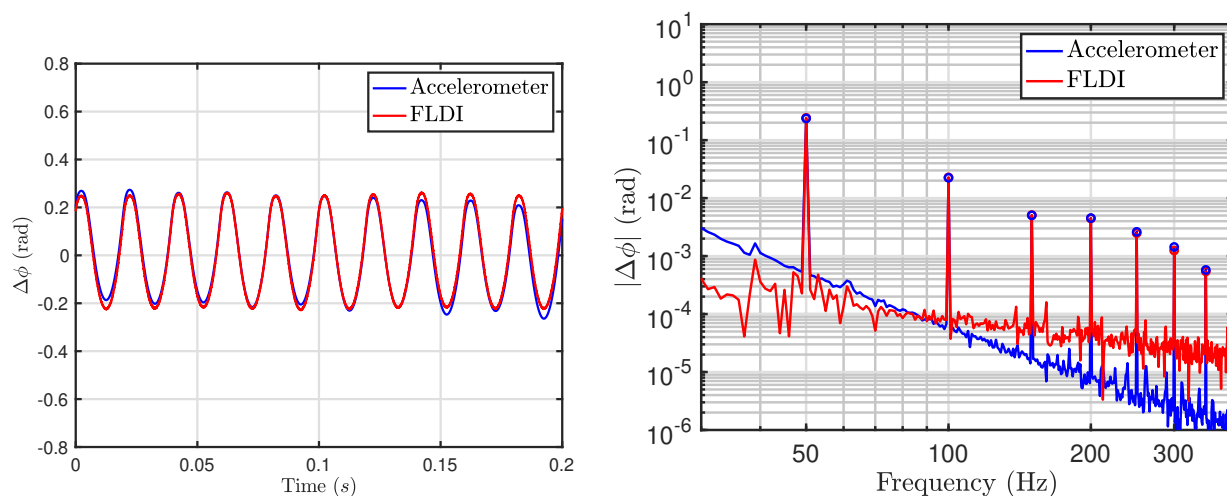
Figure 6: Phase change as measured by the accelerometer and the FLDI instrument as a function of time.

The phase object is next translated in the z-direction and comparisons are made between the response of

the accelerometer and the FLDI instrument. In Fig. 7a, from top to bottom, pictures of the FLDI beam pair are presented at z = 2.54 mm, 5.08 mm, and 7.62 mm away from the beam's focus. Correspondingly, in Fig. 7b, we present the phase change as measured by the accelerometer and the FLDI instrument at these positions. As the phase object is translated away from the focus, the increasing $1/e^2$ beam radius results in beam overlap and signal attenuation of the FLDI instrument. For example, at ± 7.62 mm away from the focus, the FLDI instrument's signal is reduced to approximately 25% of its signal at the focus. For the FLDI setup built for this experiment, this deviation from the focus represents less than 2% of the total span along which the FLDI instrument is sensitive to phase differences.

(a)

(b)
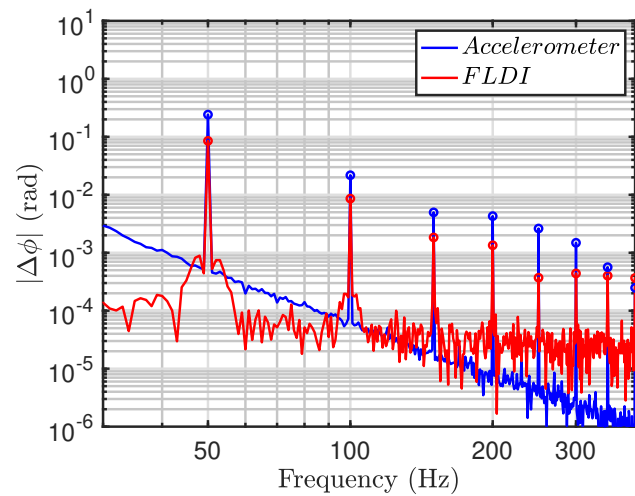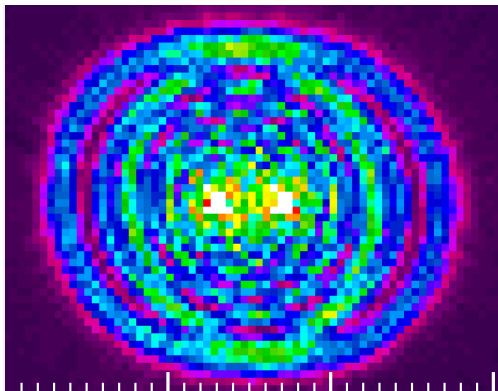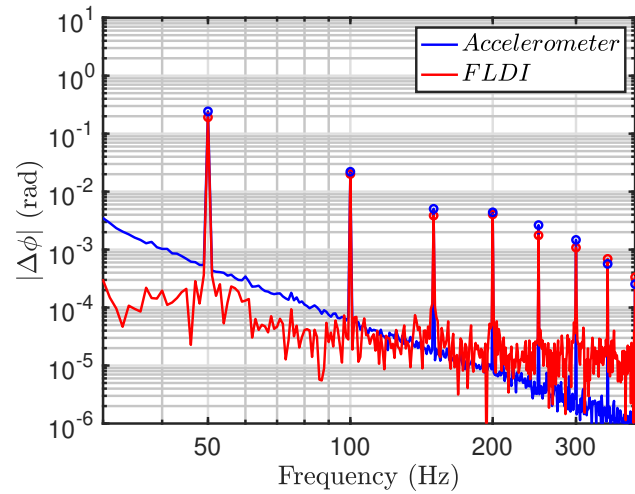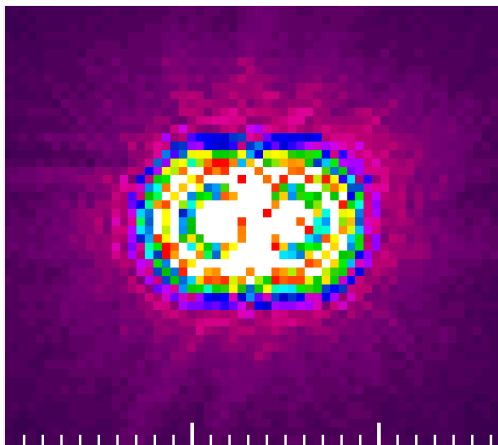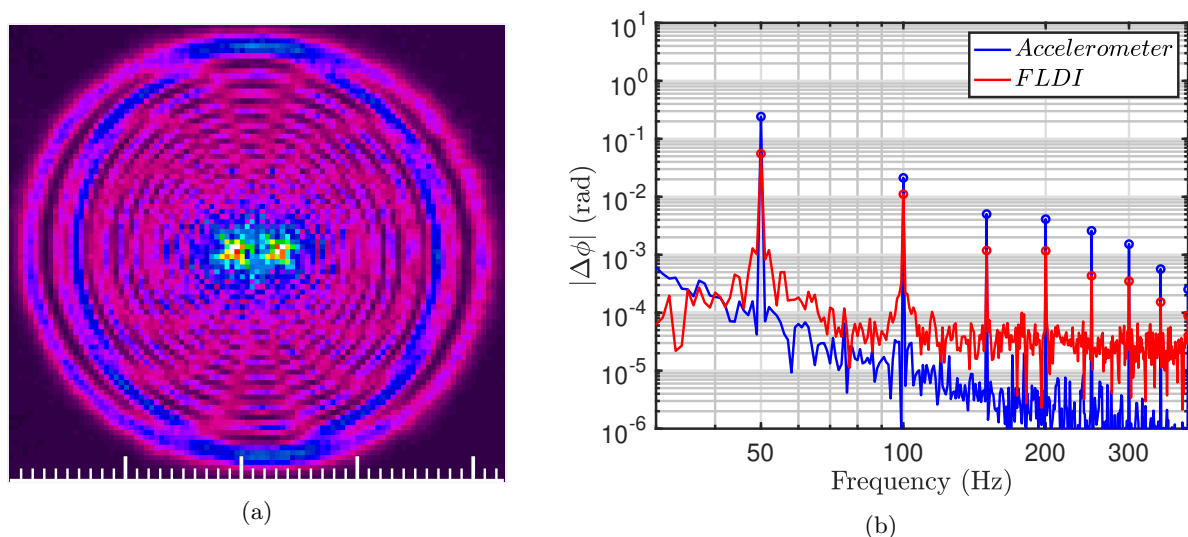
Figure 7: Phase change as measured by an accelerometer and an FLDI instrument with an f = -50 mm diverging lens used as a phase object. (a) From top to bottom: Pictures of FLDI beams taken at z = 2.54 mm, z = 5.08 mm, and z = 7.62 mm. Minor tick marks are at every 10 µm and major tick marks are at every 100 µm. (b) Comparison of $\Delta\phi$ as measured by the accelerometer and the FLDI instrument with the phase object positioned at the corresponding positions in z.

Fig. 8 summarizes the signal attenuation experienced by the FLDI instrument as the phase object is moved away from the focus. Broadband reduction in the FLDI signal is observed at increasing distances away from the focus, although no trend with frequency is readily apparent.
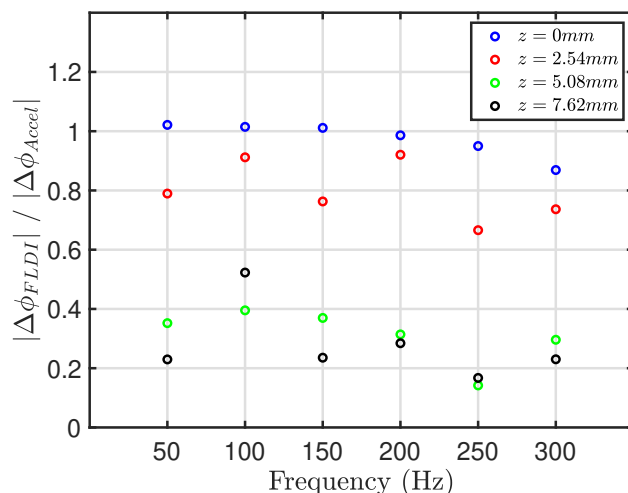
Figure 8: Ratio of the FLDI-derived phase change to accelerometer-derived phase-change with varying locations from the focus, z.

In Fig. 9, results are presented for an experiment with a D-FLDI setup, with the two beams pairs identified as FLDI A and FLDI B. A phase object in the form of a cylindrical diverging lens with a focal length of f_L =-150 mm and f_L =-400 mm is placed at the focus of the D-FLDI beams and is vibrated at a fundamental frequency of 50 Hz. The FFT shows excellent agreement between the accelerometer and the two FLDI signals in picking up the fundamental frequency and higher frequency resonances inherent to the apparatus. There is good agreement in the amplitude of the phase change between the two measurement methods noting reduced response with the lens of larger focal length (increased radius of curvature).
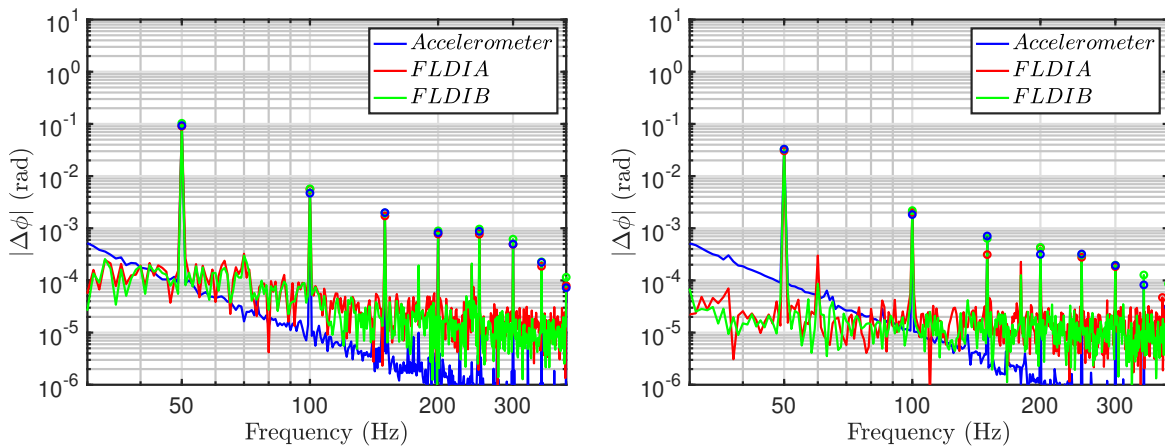
Figure 9: Comparison of accelerometer-dervied phase change to D-FLDI-derived phase change at the focus. Left: f_L =-150 mm, and Right: f_L =-400 mm.

V.   Conclusions

In this paper, we characterize an FLDI instrument by comparing its response with a prescribed phase object. The prescribed phase object was a lens placed at the FLDI focus and vibrated. Attached to this lens was an accelerometer from which displacement and, subsequently, phase change was found. This accelerometer-derived phase change was found to be in excellent agreement with FLDI-derived phase change for both the single and double FLDI setups with different focal length lenses.

Off-focus measurements with the FLDI were made with the accelerometer to act as a control. Ratios of the response show that the FLDI response is attenuated as the distance from the focus is increased. However, there is no clear sensitivity to frequency; this will be studied in subsequent work.

Acknowledgments

References

[1]Danehy, P. M., Weisberger, J., Johansen, C., Reese, D., Fahringer, T., Parziale, N. J., Dedic, C., Estevadeordal, J., and Cruden, B. A., "Non-Intrusive Measurement Techniques for Flow Characterization of Hypersonic Wind Tunnels," *Flow Characterization and Modeling of Hypersonic Wind Tunnels (NATO Science and Technology Organization Lecture Series STO-AVT 325)*, NF1676L-31725 - Von Karman Institute, Brussels, Belgium, December 3-5 2018.

[2]Smeets, G. and George, A., "Gas Dynamic Investigations in a Shock Tube using a Highly Sensitive Interferometer," Translation of isl internal report 14/71, Original 1971, Translation 1996.

[3]Smeets, G., "Laser Interferometer for High Sensitivity Measurements on Transient Phase Objects," *IEEE Transactions on Aerospace and Electronic Systems*, Vol. AES-8, No. 2, 1972, pp. 186–190. doi: 10.1109/TAES.1972.309488.

[4]Smeets, G. and George, A., "Anwendungen des Laser-Differentialinterferometers in der Gasdynamik," ISL - N 28/73, Also translated by Goetz, A.: ADA-307459, 1973.

[5]Smeets, G., "Laser-Interferometer mit grossen, fokussierten Lichtbündeln für lokale Messungen," ISL - N 11/73, 1973.

[6]Smeets, G., "Verwendung eines Laser-Differentialinterferometers zur Bestimmung lokaler Schwankungsgrössen sowie des mittleren Dichteprofils in cinem turbulenten Freistrahl," ISL - N 20/74, 1974.

[7]Smeets, G., "Flow Diagnostics by Laser Interferometry," *IEEE Transactions on Aerospace and Electronic Systems*, Vol. AES-13, No. 2, 1977, pp. 82–90. doi: 10.1109/TAES.1977.308441.

[8]Smeets, G. and George, A., "Laser Differential Interferometer Applications in Gas Dynamics," Translation of ISL Internal Report 28/73, Original 1975, Translation 1996.

[9]Azzazy, M., Modarress, D., and Hoeft, T., "High sensitivity Density Fluctuation Detector," *Proceedings of SPIE Vol. 569 High Speed Photography, Videography, and Photonics I/I*, SPIE, San Diego, CA, 1985. doi: 10.1117/12.949865.

[10]Azzazy, M., Modarress, D., and Trolinger, J. D., "Feasibility Study of Optical Boundary Layer Transition Detection Method," NASA-CR-178109, 1986.

[11]Azzazy, M., Modarress, D., and Hoeft, T., "High-sensitivity Density Fluctuation Detector," *Journal of Physics E: Scientific Instruments*, Vol. 20, No. 4, 1987, pp. 428. doi: 10.1088/0022-3735/20/4/017.

[12]O'Hare, J. E., "A Nonperturbing Boundary-Layer Transition Detector," *Proceedings of SPIE 0569, High Speed Photography, Videography, and Photonics III*, San Diego, California, 1985, pp. 58–63. doi: 10.1117/12.949864.

[13]Collicott, S. H., Schneider, S. P., and Messersmith, N. L., "Review Of Optical Diagnostic Methods For Hypersonic Low-Noise Facilities," *Proceedings of 34th Aerospace Sciences Meeting and Exhibit*, AIAA-96-0851, Reno, NV, 1996. doi: 10.2514/6.1996-851.

[14]Salyer, T. R., Collicott, S. H., and Schneider, S. P., "Feedback Stabilized Laser Differential Interferometry for Supersonic Blunt Body Experiments," *Proceedings of 38th Aerospace Sciences Meeting and Exhibit*, AIAA-2000-0416, Reno, Nevada, 2000. doi: 10.2514/6.2000-416.

[15]Parziale, N. J., Shepherd, J. E., and Hornung, H. G., "Reflected Shock Tunnel Noise Measurement by Focused Differential Interferometry," *Proceedings of 42nd AIAA Fluid Dynamics Conference and Exhibit*, AIAA-2012-3261, New Orleans, Louisiana, 25-28 June 2012. doi: 10.2514/6.2012-3261.

[16]Parziale, N. J., Jewell, J. S., Shepherd, J. E., and Hornung, H. G., "Optical Detection of Transitional Phenomena on Slender Bodies in Hypervelocity Flow," *Proceedings of RTO Specialists Meeting AVT-200/RSM-030 on Hypersonic Laminar-Turbulent Transition*, NATO, San Diego, California, 16-19 April 2012.

[17]Parziale, N. J., Shepherd, J. E., and Hornung, H. G., "Differential Interferometric Measurement of Instability at Two Points in a Hypervelocity Boundary Layer," *Proceedings of 51st AIAA Aerospace Sciences Meeting Including the New Horizons Forum and Aerospace Exposition*, AIAA-2013-0521, Grapevine, Texas, 7-10 January 2013. doi: 10.2514/6.2013-521.

[18]Parziale, N. J., Shepherd, J. E., and Hornung, H. G., "Differential Interferometric Measurement of Instability in a Hypervelocity Boundary Layer," *AIAA Journal*, Vol. 51, No. 3, 2013, pp. 750–754. doi: 10.2514/1.J052013.

[19]Parziale, N. J., *Slender-Body Hypervelocity Boundary-Layer Instability*, Ph.D. thesis, California Institute of Technology, 2013.

[20]Parziale, N. J., Shepherd, J. E., and Hornung, H. G., "Free-stream density perturbations in a reflected-shock tunnel," *Experiments in Fluids*, Vol. 55, No. 2, 2014, pp. 1665. doi: 10.1007/s00348-014-1665-0.

[21]Parziale, N. J., Shepherd, J. E., and Hornung, H. G., "Observations of hypervelocity boundary-layer instability," *Journal of Fluid Mechanics*, Vol. 781, 2015, pp. 87–112. doi: 10.1017/jfm.2015.489.

[22]Jewell, J. S., Parziale, N. J., Lam, K.-L., Hagen, B. J., and Kimmel, R. L., "Disturbance and Phase Speed Measurements for Shock Tubes and Hypersonic Boundary-Layer Instability," *Proceedings of 32nd AIAA Aerodynamic Measurement Technology and Ground Testing Conference*, AIAA-2016-3112, Washington, D. C., 13-17 June 2016. doi: 10.2514/6.2016-3112.

[23]Jewell, J. S., Hameed, A., Parziale, N. J., and Gogineni, S. P., "Disturbance Speed Measurements in a Circular Jet via Double Focused Laser Differential Interferometry," *Proceedings of AIAA Scitech 2019*, AIAA-2019-2293, San Diego, California, 7-11 January 2019. doi: 10.2514/6.2019-2293.

[24]Ceruzzi, A. P. and Cadou, C. P., "Simultaneous Velocity and Density Gradient Measurements using Two-Point Focused Laser Differential Interferometry," *Proceedings of AIAA Scitech 2019*, AIAA-2019-2295, San Diego, California, 7-11 January 2019. doi: 10.2514/6.2019-2295.

[25]Ceruzzi, A. P., Callis, B., Weber, D., and Cadou, C. P., "Application of Focused Laser Differential Interferometry (FLDI) in a Supersonic Boundary Layer," *Proceedings of AIAA Scitech 2020*, AIAA-2020-1973, Orlando, Florida, 6-10 January 2020. doi: 10.2514/6.2020-1973.

[26]Weisberger, J. M., Bathel, B. F., Herring, G. C., King, R. A., Chou, A., and Jones, S. B., "Focused Laser Differential Interferometry Measurements at NASA Langley 20-Inch Mach 6," *Proceedings of AIAA Aviation Forum*, AIAA-2019-2903, Dallas, Texas, 17-21 June 2019. doi: 10.2514/6.2019-2903.

[27]Bathel, B. F., Weisberger, J. M., Herring, G. C., King, R. A., Jones, S. B., Kennedy, R. E., and Laurence, S. J., "Two-point, parallel-beam focused laser differential interferometry with a Nomarski prism," *Applied Optics*, Vol. 59, No. 2, 2020, pp. 244–252. doi: 10.1364/AO.59.000244.

[28]Price, T. J., Gragston, M., Schmisseur, J. D., and Kreth, P. A., "Measurement of supersonic jet screech with focused laser differential interferometry," *Applied Optics*, Vol. 59, No. 28, 2020, pp. 8902–8908. doi: 10.1364/AO.402011.

[29]Hameed, A., Parziale, N. J., Paquin, L., Butler, C., and Laurence, S. J., "Hypersonic Slender-Cone Boundary Layer Instability in the UMD HyperTERP Shock Tunnel," *Proceedings of AIAA SciTech 2020*, AIAA-2020-0362, Orlando, Florida, 6-10 January 2020. doi: 10.2514/6.2020-0362.

[30]Harris, A. J., Kreth, P. A., Combs, C. S., and Schmisseur, J. D., "Laser Differential Interferometry and Schlieren as an Approach to Characterizing Freestream Disturbance Levels," *2018 AIAA Aerospace Sciences Meeting*, AIAA 2018-1100, Kissimmee, Florida, 2018. doi: 10.2514/6.2018-1100.

[31]Lawson, J. M. and Austin, J. M., "Expansion Tube Freestream Disturbance Measurements using a Focused Laser Differential Interferometer," *Proceedings of AIAA Scitech 2020*, AIAA-2020-1064, Orlando, Florida, 6-10 January 2020. doi: 10.2514/6.2020-1064.

[32]Birch, B., Buttsworth, D., and Zander, F., "Measurements of freestream density fluctuations in a hypersonic wind tunnel," *Experiments in Fluids*, Vol. 61, No. 7, 2020, pp. 1–13. doi: 10.1007/s00348-020-02992-w.

[33]Hedlund, B., Houpt, A., Gordeyev, S., and Leonov, S., "Measurement of Flow Perturbation Spectra in Mach 4.5 Corner Separation Zone," *AIAA Journal*, Vol. 56, No. 7, 2018, pp. 2699–2711. doi: 10.2514/1.J056576.

[34]Houpt, A. W. and Leonov, S. B., "Focused Laser Differential Interferometer for Supersonic Boundary Layer Measurements on Flat Plate Geometries," *Proceedings of the 2018 Plasmadynamics and Lasers Conference*, AIAA-2018-3434, Atlanta, Georgia, 25-29 June 2018. doi: 10.2514/6.2018-3434.

[35]Houpt, A. W. and Leonov, S. B., "Focused and Cylindrical-Focused Laser Differential Interferometer Characterization of SBR-50 at Mach 2," *Proceedings of AIAA Aviation 2019*, AIAA-2019-3383, Dallas, Texas, 17-21 June 2019. doi: 10.2514/6.2019-3383.

[36]Benitez, E. K., Jewell, J. S., and Schneider, S. P., "Focused Laser Differential Interferometry for Hypersonic Flow Instability Measurements with Contoured Tunnel Windows," *Proceedings of AIAA Scitech 2020*, AIAA-2020-1282, Orlando, Florida, 6-10 January 2020. doi: 10.2514/6.2020-1282.

[37]Benitez, E. K., Esquieu, S., Jewell, J. S., and Schneider, S. P., "Instability Measurements on an Axisymmetric Separation Bubble at Mach 6," *Proceedings of AIAA Aviation 2020*, AIAA-2020-3072, Virtual Event, 15-19 June 2020. doi: 10.2514/6.2020-3072.

[38]Ramprakash, A., McIntyre, T. J., Wheatley, V., and Mee, D. J., "Performance Analysis of FLDI Technique using Turbulent Jets," *Proceedings of the IX Australian Conference on Laser Diagnostics*, Adelaide, Australia, December 2-4 2019.

[39]Lawson, J. M., Neet, M. C., Grossman, I. J., and Austin, J. M., "Characterization of a Focused Laser Differential Interferometer," *Proceedings of AIAA Scitech 2019*, AIAA-2019-2296, San Diego, California, 7-11 January 2019. doi: 10.2514/6.2019-2296.

[40]Lawson, J. M., Neet, M. C., Grossman, I. J., and Austin, J. M., "Static and dynamic characterization of a focused laser differential interferometer," *Experiments in Fluids*, Vol. 61, No. 8, 2020, pp. 1–11. doi: 10.1007/s00348-020-03013-6.

[41]Fulghum, M. R., *Turbulence measurements in high-speed wind tunnels using focusing laser differential interferometry*, Ph.D. thesis, The Pennsylvania State University, 2014.

[42]Settles, G. S. and Fulghum, M. R., "The Focusing Laser Differential Interferometer, an Instrument for Localized Turbulence Measurements in Refractive Flows," *Journal of Fluids Engineering*, Vol. 138, No. 10, 2016, pp. 101402. doi: 10.1115/1.4033960.

[43]Schmidt, B. E. and Shepherd, J. E., "Analysis of focused laser differential interferometry," *Applied Optics*, Vol. 54, No. 28, 2015, pp. 8459–8472. doi: 10.1364/AO.54.008459.